Nonlinear Hysteretic Torsional Waves

J. Cabaret,[1] P. Béquin,[1] G. Theocharis,[1] V. Andreev,[2] V. E. Gusev,[1] and V. Tournat[1,*]
[1]LUNAM Universités, CNRS, Université du Maine, LAUM UMR-CNRS 6613, Avenue Olivier Messiaen, 72085 Le Mans, France
[2]Acoustics Department, Faculty of Physics, Moscow State University, 119991 Moscow, Russia
(Received 12 January 2015; published 28 July 2015)

We theoretically study and experimentally report the propagation of nonlinear hysteretic torsional pulses in a vertical granular chain made of cm-scale, self-hanged magnetic beads. As predicted by contact mechanics, the torsional coupling between two beads is found to be nonlinear hysteretic. This results in a nonlinear pulse distortion essentially different from the distortion predicted by classical nonlinearities and in a complex dynamic response depending on the history of the wave particle angular velocity. Both are consistent with the predictions of purely hysteretic nonlinear elasticity and the Preisach-Mayergoyz hysteresis model, providing the opportunity to study the phenomenon of nonlinear dynamic hysteresis in the absence of other types of material nonlinearities. The proposed configuration reveals a plethora of interesting phenomena including giant amplitude-dependent attenuation, short-term memory, as well as dispersive properties. Thus, it could find interesting applications in nonlinear wave control devices such as strong amplitude-dependent filters.

DOI: 10.1103/PhysRevLett.115.054301 PACS numbers: 43.25.+y, 45.05.+x, 45.70.-n, 46.40.Cd

Nonlinear dynamic hysteresis is involved in a wide range of acoustic effects recently observed in complex solids, often called mesoscopic solids, e.g., nonlinear softening and nonlinear absorption [1]. It is shown to originate from clapping and friction phenomena induced by acoustic waves at the internal contacts and intergrain boundaries of polycrystalline and earth materials [2–5], damaged solids [6–8], and "model" granular media [9,10]. This hysteretic nonlinearity enriches the phenomenology of the classical nonlinearity (small expansion terms of the smooth nonlinear stress-strain relation and geometric nonlinearity) with phenomena like nonlinear attenuation [2,3], memory [11], and slow dynamics [12,13].

One of the first observed manifestations of mechanical hysteresis is the shear coupling between two elastic spheres in contact [14,15]. Interestingly, periodic line assemblies of spheres, also called granular chains, have attracted growing interest in the last years for their rich nonlinear dynamics phenomena (harmonic generation, solitons, breathers, etc.) [16–21] and the potentially wide applications in wave control devices [22]. However, up to now, dynamic hysteresis has not been studied in granular chains. In addition, all the media exhibiting dynamic hysteresis (rocks, disordered granular media, concrete, composites, etc.) have been also exhibiting, at the same time, other types of nonlinearities, classical or nonclassical. Consequently, although some modeling has been proposed [23,24], it has not been possible yet to observe pulse wave distortion by purely hysteretic nonlinearity. Manifestations of hysteretic nonlinearity were observed only in narrow frequency band experiments with sine waves, via, for instance, the shift of vibration resonances [2,13] but never in the distortion of pulsed acoustic signals. The transformation of pulse profiles in media with classical quadratic nonlinearity leading to weak shock front formation of the particle velocity profile is one of the most classical observations in nonlinear acoustics [25,26]. Interestingly, the pulse distortion in media with cubic elastic nonlinearity was observed for the first time only recently [27].

In this Letter, we report for the first time the transformation of pulse profile in a medium with pure hysteretic quadratic nonlinearity, essentially different from the distortion by classical nonlinearities. We start with the observation and characterization of torsional (or pure rotational) wave propagation in a granular chain composed of identical magnetic spheres. Because of the pure torsional coupling at the contacts excited in a rotational motion around the z axis of the chain, pure nonlinear hysteretic behavior is observed. The latter is quantitatively characterized for a single contact in a resonance experiment and then used for the modeling of torsional wave pulse distortion by quadratic hysteresis. A quantitative comparison with the experimental distorted pulse profiles in a chain of 70 beads shows the validity of the developed modeling. Extremely large nonlinear self-action (including self-attenuation and pulse deceleration) is demonstrated for parts of the pulse profile, depending on the previous loading by the pulse itself (a short-term memory).

Experimental configuration.—The medium is composed of 15 to 70 magnetic beads of diameter $d = 2R = 19$ mm and mass $m = 27$ g [see Fig. 1(a)] [28,29]. The magnetic poles of the beads are aligned along the chain (z axis) and provide a magnetic force $F_0 = 54$ N between beads, normal to the contacts. F_0 exceeds largely the gravity force, and, thus, the contact forces along the chain are considered identical in this study. The chain is excited at the

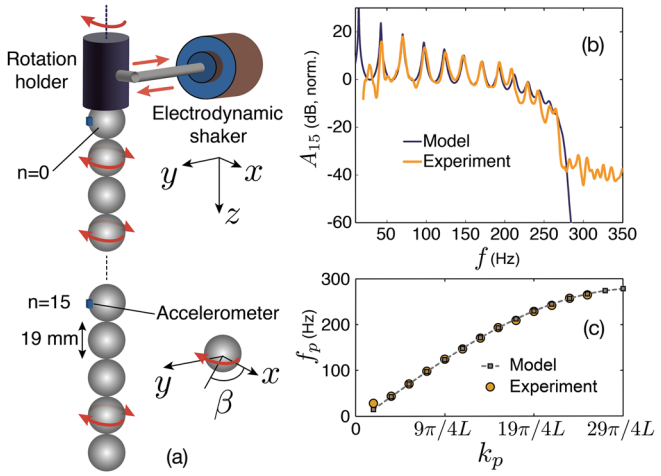

FIG. 1 (color online). (a) Experimental configuration for the torsional wave propagation (pure rotation of the beads around the z axis of the chain). (b) Signal acceleration at bead 15 versus frequency for a 15-bead chain. (c) Dispersion relation retrieved from the p resonance frequencies of the chain.

top by a shaker (B&K 4810) coupled to the side of a circular ball-bearing system, which produces a rotational motion relative to the z axis of the chain [30]. This dynamic rotation is transmitted along the chain thanks to the torsional rigidity of the contacts, leading to torsional wave propagation. For detecting the waves, accelerometers (type PCB 352C23) are glued to the side of several beads, and angular particle accelerations are recorded via an oscilloscope or a spectrum analyzer.

The dynamics of the chain can be described through the following system of equations of rotational motion for each bead n interacting with its nearest neighbors $n-1$ and $n+1$ through torsional moments,

$$J\frac{\partial^2\beta_n}{\partial t^2} = M_n - M_{n-1}, \tag{1}$$

where β_n is the rotation angle of bead n, $J = 2mR^2/5 \simeq 9.85\times10^{-7}$ kg m^2 is the moment of inertia of the beads, t the time, and M_n the nonlinear torsional moment depending on the relative rotation angle between beads $n+1$ and n. Following the approach in Refs. [14,30,34], the moment-angle relationship for oscillatory motion (a simple periodic driving) between two spheres in contact can be approximated by linear and quadratic hysteretic functions (see the Supplemental Material [30]),

$$M_n = M_n^{\mathrm{lin}} + M_n^h = K_t\left\{\psi_n - h\left[\psi_n^*\psi_n + \frac{1}{2}(\psi_n^2 - \psi_n^{*2})\mathrm{sgn}(\dot{\psi}_n)\right]\right\}, \tag{2}$$

where $\psi_n = \beta_{n+1} - \beta_n$ is the relative rotation angle between two adjacent beads, ψ_n^* is its magnitude, $K_t = d(1-\nu)F_0$ is the linear torsional constant, $h = Ea^2/(1+\nu)\mu F_0$ is defined as the parameter of quadratic hysteretic nonlinearity, with μ the *a priori* unknown friction coefficient of the bead's material, $E = 160$ G Pa the Young's modulus, $\nu \simeq 0.24$ the Poisson ratio of the bead's material, and $a = [3F_0R(1-\nu^2)/4E]^{1/3} \simeq 130$ μm the contact radius.

In Fig. 1(b), the angular particle acceleration A_{15} of bead $n = 15$ is presented versus frequency in the case of a 15-bead chain. In this finite-length chain, resonances are observed up to the cutoff frequency $f_c \simeq 275$ Hz above which the waves are evanescent. Simulating the linear dynamics of the chain with springs having a complex constant $K_t = 0.78(1+0.027i)$ N m to fit the experimental losses, we obtain the theoretical curve in Fig. 1(b). The theoretical cutoff frequency $f_c = \sqrt{K_t/J}/\pi = 283$ Hz is found to be in good agreement with the experimental one. From the experimental resonance frequencies f_p (with $p = 1,\ldots,15$) of the finite chain, the dispersion relation can be retrieved. At the p-order resonance of the chain, the wave number is $k_p = (2p-1)\pi/4L$, where L is the length of the chain. The relation $f_p - k_p$ is also derived for the simulation results, and the two dispersion curves are compared successfully in Fig. 1(c). These observations provide an estimate of the long-wavelength torsional wave velocity in such system $c = d\sqrt{K_t/J} \simeq 17$ m/s.

To verify in our configuration the validity of the nonlinear moment-angle relationship (2) and to estimate the parameter h, we characterize a single contact between two spheres in a nonlinear resonance experiment as depicted in Fig. 2(d). The downshift of the resonance frequency with a linear dependence on the oscillation amplitude can be attributed to hysteretic quadratic

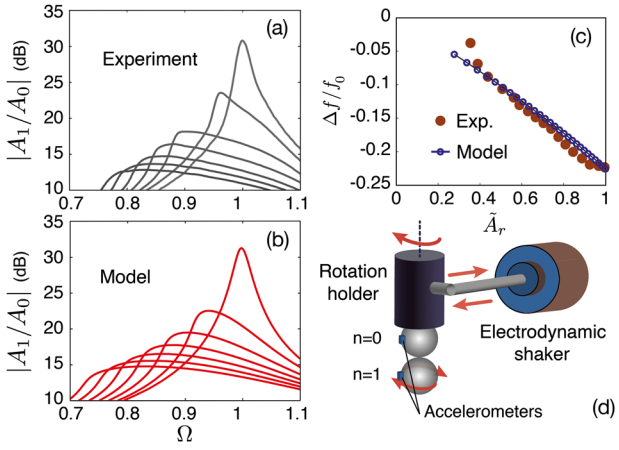

FIG. 2 (color online). Magnitude of the acceleration transfer function (detected acceleration A_1 at bead 1 over the acceleration A_0 at bead 0) of a "two-beads–one-contact" system for different excitation levels, experiment (a) and theory (b). (c) Relative resonance frequency shift as a function of the detected resonance amplitude (normalized to the one at the maximum excitation level). (d) Setup for the single contact characterization in torsion.

nonlinearity [2–5], while the shift proportional to the square of the amplitude at the lowest excitation levels can be attributed to either the cubic elastic nonlinearity [35–37] or to the hysteretic nonlinearity described by the Preisach-Arrhenius model [38].

In Fig. 2(a), the experimental ratio between acceleration signals at bead 0 and bead 1 is shown as a function of normalized frequency $\Omega = f/f_0$, where $f_0 = 159$ Hz is the experimental resonance frequency at the smallest excitation amplitude. A downward resonance frequency shift is observed as well as a nonlinear attenuation process [2,3]. The relative resonance frequency shift $\Delta f/f_0 = (f_r - f_0)/f_0$ is shown to scale linearly with the detected resonance amplitude in Fig. 2(c), which is consistent with quadratic hysteresis. For comparison, the theoretical transfer function obtained with the harmonic balance method for the moment-angle relationship Eq. (2) and neglecting contributions from higher harmonics [39,40] is plotted in Fig. 2(b). A quantitative agreement between the theoretical and experimental resonance curves and resonance frequency shifts is obtained for $h \simeq 258 \pm 16$ (which corresponds to a realistic friction coefficient $\mu \simeq 0.32 \pm 0.02$). The fitted quality factor $Q_0 = 37$ is also in agreement with the imaginary part of K_t used above.

After having extracted the linear properties of the medium and tested the quadratic hysteretic behavior for a single contact, we turn to the nonlinear propagation of torsional wave pulses. In order to avoid simultaneous detection of forward and backward propagating waves and to mimic a semi-infinite chain, we use a 70-bead-long chain. The detector is placed at the bead $n = 18$, and the wave propagates through 104 beads before coming back to the receiver after reflection by the free boundary. The pulse central frequency should be sufficiently low to avoid strong dispersion effects occurring at frequencies close to the Bragg frequency $f_c \simeq 275$ Hz but also sufficiently high to limit its spatial extent and be able to distinguish incident from reflected pulses. Therefore, a central frequency of 100 Hz has been chosen. The first bead velocity is shown in Fig. 3, corresponding to the time-integrated accelerometer signal.

We describe the pulse distortion starting from the following evolution equation valid for any type of signal in a one-dimensional dispersionless medium where linear dissipation is neglected [23,24,40,41],

$$\frac{\partial \bar{\theta}_v}{\partial \xi} - \frac{1}{2}\frac{\partial \bar{M}_h}{\partial \bar{\theta}_v}\frac{\partial \bar{\theta}_v}{\partial \tau} = 0. \tag{3}$$

Here, in accordance with the considered problem, $\bar{\theta}_v = \theta_v/\theta_0$ is the normalized angular particle velocity, θ_0 is the angular velocity amplitude of the first phase of the emitted wave packet at $z=0$, $\tau = (t - z/c)/t_0$ where $t_0 = 5.77$ ms is the duration of the first phase of the emitted signal, $\bar{M}_h = M_h/(dK_t)$, and $\xi = z/z_{\rm nl}$ with $z_{\rm nl} = c^2 t_0/hd\theta_0$ the characteristic nonlinear length [42].

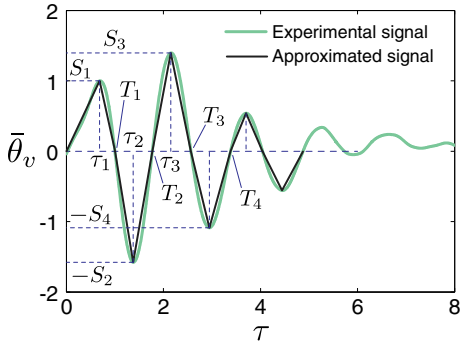

FIG. 3 (color online). Experimental angular particle velocity $\bar{\theta}_v = \theta_v/\theta_0$ at bead 1 for the smallest excitation amplitude and its approximation by a linear piecewise function. T_n's are the positions of the signal zeros in time normalized by $t_0 = 5.77$ ms so that $T_1 = 1$, τ_n's are the extrema positions in time, and S_n's are the extrema amplitudes normalized by θ_0 so that $S_1 = 1$.

The important term $\partial \bar{M}_h/\partial \bar{\theta}_v$ having the physical sense of a normalized amplitude-dependent modulus [23,24,43] and containing the hysteretic behavior has been analytically derived from the Preisach-Mayergoyz (PM) model of hysteresis [1,44,45]. This phenomenological model developed initially in magnetism and then adapted to elastic waves considers a large number of hysteretic elements (hysterons), each having two possible stress states. The transitions from one state to another take place at two characteristic strains, one for each sign of the strain rate. A hysteretic medium can be represented via a distribution of hysterons in the PM plane formed by two axes whose coordinates are the two characteristic strains of the hysterons. Unlike existing analytical formulas for the quadratic hysteresis, this model has the ability to model the instantaneous memory stored in the hysterons' states under the action of an arbitrary varying acoustic loading and, thus, is applicable to arbitrary signals such as the pulses observed here.

The evolution equation (3) is then modified into a system of equations derived for the linear piecewise approximated signal of Fig. 3. The derivation using the PM model of hysteresis is detailed in the Supplemental Material [30] and leads to the following system,

$$dT_n = S_n d\xi/2, \tag{4}$$

$$d\tau_n = (T_n - \tau_n)A_n d\xi/(T_n - T_{n-1}), \tag{5}$$

$$dS_n = -A_n S_n d\xi/(T_n - T_{n-1}), \tag{6}$$

with $A_n = S_n$ if $S_n > S_{n-1}$ and $A_n = (S_n + S_{n-1})/2$ if $S_n < S_{n-1}$. The system (4)–(6) describes, respectively, the small shifts of the positions in time of the zeros (dT_n), the extrema of the signal ($d\tau_n$), as well as the change in extremal values (dS_n) when a small change in $d\xi$ occurs, i.e., either a small distance or a small excitation amplitude

change. So, by increasing step by step the amplitude ξ, the system (4)–(6) describes the distortion by the hysteretic nonlinearity of the linear piecewise approximated pulse. We note here that the evolution of the parameters of the signal phase number n depends, in general, on phases n and $n-1$ but not on previous $(n-2, n-3, \ldots)$, i.e., a short-memory effect. Equations (4) and (5) have a clear physical sense. The local time delays $(dT_n, d\tau_n)$ are proportional to wave amplitudes (S_n, A_n) as it could be expected for quadratic hysteretic nonlinearity [1]. Equation (6) describes local nonlinear absorption with an absorption coefficient proportional to the wave amplitude and to the local "frequency" (inverse duration of the pulse phase $T_n - T_{n-1}$), also theoretically expected for quadratic hysteretic nonlinearity [13].

In Fig. 4(a), we plot the experimental angular velocity signals for different excitation amplitudes at bead 1 ($z = 0$ so by definition $\xi = 0$) and at bead 18 ($z = 18d = 0.323$ m), i.e., for different values of ξ. For the smallest excitation amplitude, the characteristic angular velocity is $\theta_0 \simeq 0.17$ rad/s and the experimentally found speed of sound is $c = 20$ m/s. As observed and

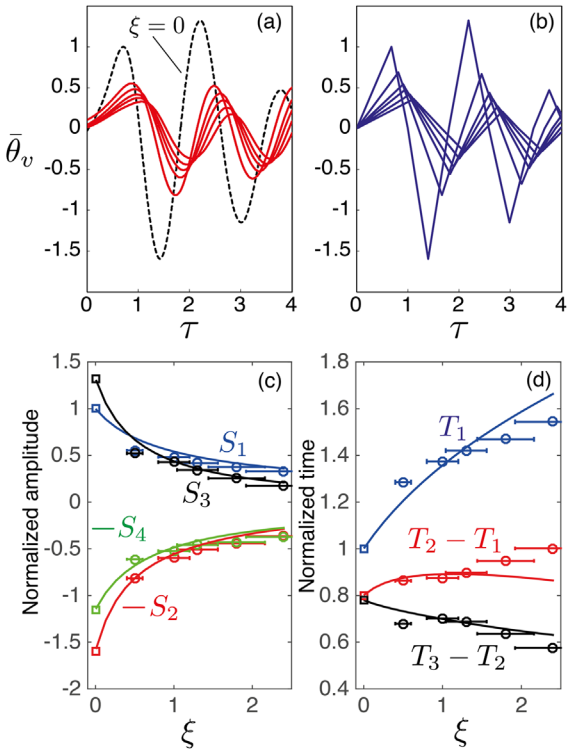

FIG. 4 (color online). (a) Experimental angular velocity signals for different values of ξ: at bead 1 ($\xi = 0$ dashed line) and at bead 18 for different excitation amplitudes ($\xi = 0.5$, 1, 1.3, 1.8, and 2.4 for $h = 800$). (b) Corresponding theoretical angular velocity signals. (c) Experimental (symbols) and theoretical (lines) amplitudes of the four first signal extrema versus ξ. (d) Experimental (symbols) and theoretical (lines) durations of the three first signal phases versus ξ. Error bar limits represent simulated results for $h = 640$ and 960.

predicted for waves in resonance experiments [2–5,13], both effects of nonlinear softening and nonlinear attenuation are manifested here for the multiphase pulses. In particular, in Figs. 4(a) and 4(b), one can clearly observe that increasing ξ, the pulse extrema S_n arrive later (nonlinear softening) and decrease in amplitude (nonlinear attenuation). Additionally, in connection with the short-memory effect, it is striking to observe that different parts of the signal are not attenuated in the same way. For instance, the third extremum is attenuated faster than the first ($|dS_3| > |dS_1|$), although starting from $\xi = 0.5$, $S_3 \simeq S_1$ [see Fig. 4(c)]. This effect is explained by Eq. (6) where the evolution of signal extrema values dS_n shows a dependence on the inverse duration of the pulse phase $T_n - T_{n-1}$ and from the fact that for the experimental signal under consideration $T_3 - T_2 < T_1$ [see Fig. 4(d)]. An important role is also played by the memory effect, because while the dynamics of the first phase duration T_1 depends only on its amplitude S_1, Eq. (4), and T_1 is continuously growing, the variation of the third phase duration $T_3 - T_2$ depends on the difference between its amplitude S_3 and the amplitude of the previous phase S_2 (short-term memory effect), and it diminishes because $S_3 < S_2$ [see Fig. 4(d)]. For $h = 800 \pm 160$, all these observations, Figs. 4(c) and 4(d), are quantitatively captured by the modeled signal distortion from Eqs. (4)–(6). This value of the parameter of hysteretic nonlinearity is different from the one evaluated above for the one-contact–one-bead system resonance $h \simeq 258$, although of the same order of magnitude. This deviation could be attributed to the differences in the setup (chain of two beads versus 70 beads) through the role of the weight, to the possibly different contact wears and their expected important influence on h through the friction coefficient μ but also to the possible slight misalignment of the magnetic beads that could introduce forces and moments that are not intrinsically represented in the model.

Conclusions.—Existence and propagation of pure torsional waves in a granular magnetic chain were reported. The torsional waves showed dispersive properties associated to the periodicity of the medium. Through a single contact nonlinear resonance experiment, we verified a nonlinear quadratic hysteretic relationship for the moment angle (equivalent to stress strain). Following this observation, we developed a set of equations based on the PM model of hysteresis to describe the torsional pulse propagation. The model's results compare very well with experimental distorted pulses observed for increasing excitation amplitude in a 70-bead-long chain. The reported nonlinear transformation of pulse profile in a medium with hysteretic quadratic nonlinearity essentially extends the historically observed distortion by quadratic nonlinearity [25] and the more recently observed distortion by cubic nonlinearity [27].

In particular, we found a giant nonlinear attenuation (or shift in time) for each phase of the pulse, which depends on

the characteristics (amplitude, duration, etc.) of the particular phase of the signal and sometimes on the relative amplitudes of the previous phases. This signifies a short-term wave-memory effect. The observed giant nonlinear attenuation effects and the short-term memory could become key components of nonlinear elastic wave control devices [18,46,47]. Moreover, the presented configuration could be used as a model medium to study fundamental nonlinear wave processes, e.g., frequency mixing, interaction of counterpropagating waves, and self-modulation instability still unexplored for hysteretic nonlinearity.

*Corresponding author.
vincent.tournat@univ-lemans.fr

[1] R. A. Guyer and P. A. Johnson, *Nonlinear Mesoscopic Elasticity* (Wiley-VCH, New York, 2009).
[2] V. E. Nazarov, L. A. Ostrovsky, I. A. Soustova, and A. M. Sutin, Sov. Phys. Acoust. **34**, 284 (1988).
[3] V. E. Nazarov, L. A. Ostrovsky, I. A. Soustova, and A. M. Sutin, Phys. Earth Planet. Inter. **50**, 65 (1988).
[4] R. A. Guyer and P. A. Johnson, Phys. Today **52**, 30 (1999).
[5] R. A. Guyer, J. TenCate, and P. Johnson, Phys. Rev. Lett. **82**, 3280 (1999).
[6] I. Y. Solodov and B. A. Korshak, Phys. Rev. Lett. **88**, 014303 (2001).
[7] A. Moussatov, V. Gusev, and B. Castagnede, Phys. Rev. Lett. **90**, 124301 (2003).
[8] K. E. A. Van den Abeele, P. A. Johnson, and A. Sutin, Res. Nondestr. Eval **12**, 17 (2000).
[9] C. Inserra, V. Tournat, and V. Gusev, Appl. Phys. Lett. **92**, 191916 (2008).
[10] P. A. Johnson and X. Jia, Nature (London) **437**, 871 (2005).
[11] K. R. McCall and R. A. Guyer, J. Geophys. Res. **99**, 23887 (1994).
[12] J. A. TenCate and T. J. Shankland, Geophys. Res. Lett. **23**, 3019 (1996).
[13] P. A. Johnson and A. Sutin, J. Acoust. Soc. Am. **117**, 124 (2005).
[14] K. L. Johnson, *Contact Mechanics*, 2nd ed. (Cambridge University Press, Cambridge, England, 1985).
[15] R. D. Mindlin, W. P. Mason, T. F. Osmer, and H. Deresiewicz, Proc. 1st Natl. Congr. Appl. Mech. **203** (1952).
[16] V. F. Nesterenko, *Dynamics of Heterogeneous Materials* (Springer, New York, 2001).
[17] J. Cabaret, V. Tournat, and P. Béquin, Phys. Rev. E **86**, 041305 (2012).
[18] N. Boechler, G. Theocharis, S. Job, P. G. Kevrekidis, M. A. Porter, and C. Daraio, Phys. Rev. Lett. **104**, 244302 (2010).
[19] S. Sen, J. Hong, J. Bang, E. Avalos, and R. Doney, Phys. Rep. **462**, 21 (2008).
[20] S. Job, F. Melo, A. Sokolow, and S. Sen, Phys. Rev. Lett. **94**, 178002 (2005).
[21] J. Lydon, G. Theocharis, and C. Daraio, Phys. Rev. E **91**, 023208 (2015).
[22] N. Boechler, G. Theocharis, and C. Daraio, Nat. Mater. **10**, 665 (2011).
[23] V. Gusev, J. Acoust. Soc. Am. **107**, 3047 (2000).
[24] V. E. Gusev and V. Aleshin, J. Acoust. Soc. Am. **112**, 2666 (2002).
[25] J. S. Mendousse, J. Acoust. Soc. Am. **25**, 51 (1953).
[26] *Nonlinear Acoustics*, edited by M. F. Hamilton and D. T. Blackstock (Academic Press, New York, 1997).
[27] S. Catheline, J.-L. Gennisson, M. Tanter, and M. Fink, Phys. Rev. Lett. **91**, 164301 (2003).
[28] http://www.supermagnet.com.
[29] F. J. Sierra-Valdez, F. Pacheco-Vázquez, O. Carvente, F. Malloggi, J. Cruz-Damas, R. Rechtman, and J. C. Ruiz-Suárez, Phys. Rev. E **81**, 011301 (2010).
[30] See the Supplemental Material at http://link.aps.org/supplemental/10.1103/PhysRevLett.115.054301, for details on the dynamic moment-angle relationship derivation, the modeling of the hysteretic distortion, and the experiments, which includes Refs. [14,15,31–33].
[31] R. D. Mindlin, J. Appl. Mech. **71**, 259 (1949).
[32] J. L. Lubkin and P. H. McDonald, J. Appl. Mech. **18**, 183 (1951).
[33] M. Hetényi and P. H. McDonald, J. Appl. Mech. **25**, 396 (1958).
[34] H. Deresiewicz, J. Appl. Mech. **21**, 52 (1954).
[35] A. S. Nowick, Phys. Rev. **80**, 249 (1950).
[36] V. E. Nazarov, A. V. Radostin, and I. A. Soustova, Acoust. Phys. **48**, 76 (2002).
[37] J. A. TenCate, D. Pasqualini, S. Habib, K. Heitmann, D. Higdon, and P. A. Johnson, Phys. Rev. Lett. **93**, 065501 (2004).
[38] V. Gusev and V. Tournat, Phys. Rev. B **72**, 054104 (2005).
[39] A. H. Nayfeh and T. Mook, *Nonlinear Vibrations* (John Wiley, New York, 1979).
[40] V. Gusev, J. Acoust. Soc. Am. **117**, 1850 (2005).
[41] V. Gusev, Wave Motion **42**, 97 (2005); **33**, 145 (2001).
[42] Note here that due to the proportionality between the angular particle velocity $\bar{\theta}_v$ and the angular strain, the profiles of these quantities are the same, and their evolution is described by Eq. (3).
[43] V. Aleshin, V. Gusev, and V. Zaitsev, Ultrasonics **42**, 1053 (2004).
[44] F. Preisach, Z. Phys. **94**, 277 (1935).
[45] I. D. Mayergoyz, Phys. Rev. Lett. **56**, 1518 (1986).
[46] F. Li, P. Anzel, J. Yang, P. Kevrekidis, and C. Daraio, Nat. Commun. **5**, 5311 (2014).
[47] J. Yang, S. Dunatunga, and C. Daraio, Acta Mech. **223**, 549 (2012).